

Review

Electronic State of Fe⁴⁺ Ions in Perovskite-Type Oxides

Mikio TAKANO* and Yasuo TAKEDA**

Received October 30, 1983

Our Mössbauer effect studies on the electronic state of Fe⁴⁺ ions in perovskite-type oxides, Ca_{1-x}Sr_xFeO₃ (0 ≤ x ≤ 1), Sr_{1-y}La_yFeO₃ (0 ≤ y ≤ 0.6), and some others, are summarized and discussed. The Fe⁴⁺ ions take a high spin state, t_{2g}³e_g¹, and the e_g electrons are accommodated in a narrow σ* band. The quarter-filled σ* band state is stable down to the lowest temperature in SrFeO₃. However, when the Sr-content is enough decreased, the e_g electrons get localized at low temperatures in a special way to form a mixed valence state, that is, a charge disproportionation of the Fe⁴⁺ ions into Fe³⁺ (t_{2g}³e_g²) and Fe⁵⁺ (t_{2g}³) ions which can be seen typically in CaFeO₃ and Sr_{0.7}La_{0.3}FeO₃. In the intermediate composition ranges of 0 < x < 1 and 0 < y < 0.3 quite unusual intermediate states are realized and, hence, the chemical formulas of these oxides at low temperatures can be expressed conveniently as Ca_{1-x}Sr_xFe_{0.5}^(3+d)Fe_{0.5}^(5-d)O₃ and Sr_{1-y}La_yFe_{(1+y)/2}^(3+δ)Fe_{(1-y)/2}^(5-δ)O₃.

KEY WORDS: Perovskite/ Fe⁴⁺/ Fe⁵⁺/ Charge Disproportionation/
Mössbauer Effect/

1. INTRODUCTION

An Fe atom has six 3d electrons and two 4s electrons in its neutral state and, therefore, can take various ionic valence states of 1+ to 8+ by releasing these electrons. However, the valence states stabilized in oxides are, at the present stage, limited to from 2+ to 6+. These ions are rather small in size and can be suitably accommodated in oxygen-polyhedra such as octahedra and tetrahedra. The numbers of oxides containing Fe²⁺ and/or Fe³⁺ ions are very large, and some of them have been very useful to our daily life. For example, α-Fe₂O₃ exhibits various tones of reddish color depending on the particle size and can be used as a pigment. γ-Fe₂O₃ with a metal-deficient spinel structure is ferrimagnetic and is a useful magnetic recording material. On the other hand, the numbers of oxides containing highly charged ions, Fe⁴⁺ to Fe⁶⁺ ions, are very small because these valence states are stabilized under strongly oxidizing conditions. We have been interested in perovskite-type oxides containing Fe⁴⁺ ions for the last several years. The behavior of d electrons changes in a very interesting way depending on temperature, oxygen deficiency, and also on such cations as Sr and Ca coexisting with iron in the same crystal. We summarize and discuss the experimental results in this paper, hoping that these oxides also become useful. In fact some investigators are now trying to

* 高野幹夫: Laboratory of Solid State Chemistry, Institute for Chemical Research, Kyoto University, Uji, Kyoto 611.

** 武田保雄: Department of Chemistry, Faculty of Engineering, Mie University, Tsu 514.

apply these oxides to gas sensors, catalysts, and electrodes, and so on.

Table I presents representative Fe⁴⁺-oxides of compositions close to stoichiometry.¹⁻⁷⁾ It is characteristic that all of them contain both comparatively large

Table I. Representative Oxides Containing Fe⁴⁺ Ions.

Oxide	Structure
SrFeO ₃ ¹⁾	cubic, perovskite-type
CaFeO ₃ ^{2,3)}	cubic, perovskite-type tetragonal,
Sr ₃ Fe ₂ O _{6.9} ⁴⁾	tetragonal, Sr ₃ Ti ₂ O ₇ -type
Sr ₂ FeO _{3.7} ⁵⁾	tetragonal, K ₂ NiF ₄ -type
Sr _{0.5} La _{1.5} Li _{0.5} Fe _{0.5} O ₄ ⁶⁾	tetragonal, K ₂ NiF ₄ -type
BaFeO _{2.95} ⁷⁾	hexagonal, 6H BaTiO ₃ -type

alkaline earth cations and small Fe⁴⁺ ions. These phases have generally been obtained by treating the corresponding oxygen-deficient phases under high oxygen pressures at suitable temperatures. MacChesney *et al.*¹⁾ reported in 1965 to have successfully obtained stoichiometric SrFeO₃ by annealing SrFeO_{3- δ} under an oxygen pressure (Po₂) of 89MPa for one week at 628K, while slightly oxygen-deficient Sr₃Fe₂O_{6.9} was formed under quite similar conditions of an Po₂ of 96MPa at 673K.⁴⁾ If it is assumed that Fe³⁺ ions are formed by oxygen-deficiency, this composition corresponds to a ratio of Fe³⁺/Fe⁴⁺=1/9. A much higher oxygen pressure of 2GPa was applied to CaFeO_{2.5} at 1273K to prepare CaFeO₃.³⁾

By the way, Ichida's works⁸⁾ are quite characteristic with respect to the starting materials. He prepared SeFeO₄ and BaFeO₄ by a wet method; they were thermally decomposed under controlled oxygen pressures. Though the decomposition products did not include the corresponding stoichiometric perovskite phases because of the insufficient oxygen pressure, the use of fine powders of highly decomposable oxygen-excess materials made it possible to find some new oxygen-deficient equilibrium phases, stable only at relatively low temperatures.

Among the oxides listed in Table I, SrFeO₃ and CaFeO₃ have been studied most intensively because these are stoichiometric, take the simplest structure, and are in remarkable contrast with each other with respect to the behavior of d electrons. We have concentrated our interest on these and related perovskite-type oxides, and the structure will be illustrated below.

The ideal perovskite structure include two kinds of cations, M(I) and M(II), the former having the same size as the O²⁻ anion's and the latter just fitting oxygen-octahedral voids. The cubic unit cell with the M(II) ions located at its corners is illustrated in Fig. 1. [M(II)O₆] octahedra are linked along the cubic axes by sharing their corners. For example, SrFeO₃ keeps cubic symmetry down to at least 4K.¹⁾ The lattice constant, *a*, at room temperature is 0.3850 nm. According to Shannon,⁹⁾ the effective ionic radius for a Sr²⁺ ion coordinated by twelve O²⁻

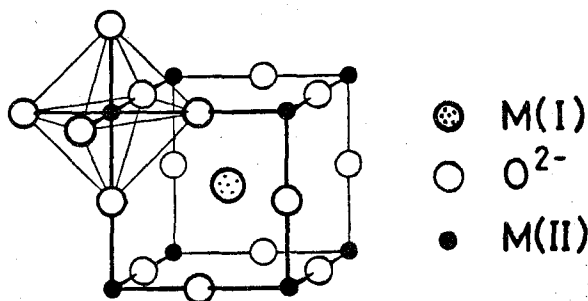


Fig. 1. Unit cell of the perovskite structure.

ions, $r(\text{XII Sr}^{2+})$, is 0.144 nm and that of an octahedrally coordinated Fe^{4+} ion, $r(\text{VI Fe}^{4+})$, is 0.585 nm when $r(\text{VI O}^{2-}) = 0.140$ nm is assumed.

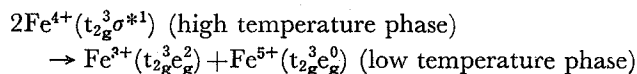
2. ELECTRONIC STATE^{10,11)}

When a transition metal ion is located at the center of an oxygen octahedron, the fivefold-degenerate d orbitals are split into twofold-degenerate orbitals of e_g symmetry and threefold-degenerate orbitals of t_{2g} symmetry. The octahedral crystal field and covalent mixing with the anionic p orbitals make the e_g orbitals energetically unfavorable by $10D_q$ in comparison with the t_{2g} 's. An Fe^{4+} ion has four 3d electrons, and two kinds of electronic configurations are possible: one is the high spin state, $t_{2g}^3 e_g^1$, and the other is $t_{2g}^4 e_g^0$, the low spin state. The latter state is stabilized at the expense of intra-atomic exchange interaction when $10D_q$ is large enough.

When $[\text{M(II)O}_6]$ octahedra are linked to form perovskite structure, a stabilization of the electronic state by a virtual transfer of d electrons from one transition metal ion to near-neighboring metal ions should be taken into account. Such a transfer via an intervening anion is, generally, more important as the covalent mixing of the relevant metallic and anionic orbitals is larger. However, the electron-electron Coulomb energy at the neighboring M(II) ions is increased. So, two kinds of typical d electron states can be assumed. One is an itinerant state with a broad energy band to accommodate the d electrons. The crystal tends to keep high symmetry to maintain the strong orbital overlapping. A typical example is LaNiO_3 . The Ni^{3+} ion is in the low spin state of $t_{2g}^6 e_g^1$. The σ^* band is formed from the crystal-field $e_g(\text{Ni}^{3+})$ orbitals containing the $p_o(\text{O}^{2-})$ orbitals. The broadened, quarter-filled σ^* band gives metallic conductivity and Pauli paramagnetism. The other is a localized state. The metal ions keep their localized magnetic moments, and the conductivity is semiconductive. Moreover, if the ground state is orbital-degenerate, the degeneracy may be lifted by distorting the surrounding oxygen-octahedron according to the Jahn-Teller effect. LaMnO_3 is a typical example. The Mn^{3+} ion takes the high spin state of $t_{2g}^3 e_g^1$, and the cooperative crystalline distortion to orthorhombic symmetry occurs at about 880K.

LaMnO_3 and LaNiO_3 are, thus, in good contrast with respect to their e_g electrons. Studies on SrFeO_3 , CaFeO_3 , and some related oxides have shown that the Fe^{4+} ion also has a single electron in the two-fold e_g orbitals which form a narrow

σ^* band (*i.e.* the high spin state) and that the behavior of the e_g electron can be characterized aptly by a disproportionation of the Fe⁴⁺ ions into Fe³⁺ and "Fe⁵⁺" ions, *i.e.*



3. SrFeO₃ AND CaFeO₃

3.1. SrFeO₃

The properties of SrFeO₃ will be summarized and discussed below. The electrical resistivity measured on a sintered body is rather low, $\sim 10^{-3} \Omega \text{ cm}$, and almost temperature independent.¹⁾ This suggests the existence of itinerant d electrons. Magnetic susceptibility¹⁾ and neutron diffraction¹²⁾ measurements revealed that this oxide is an antiferromagnet having a screw spin structure with a propagation vector parallel to the $\langle 111 \rangle$ direction ($T_N=134\text{K}$). The angle between the magnetic moments of the nearest-neighboring Fe ions is only about 40°. The magnetic exchange interactions estimated from a paramagnetic neutron-scattering measurement¹³⁾ range from the ferromagnetic nearest-neighbor interaction of $J_1=1.2 \text{ meV}$ to the antiferromagnetic second- and fourth-nearest-neighbor interactions of $J_2=-0.1 \text{ meV}$ and $J_4=-0.3 \text{ meV}$. The coexistence of these interactions of opposite signs results in the special type of spin structure.

The magnitude of magnetic moment can be the key to an understanding of the electronic state. An estimation by neutron techniques is, however, rather complicated: two research groups have reported different values. Takeda *et al.*¹³⁾ made a measurement on a powdered SrFeO₃ sample and obtained a value of $\mu_{\text{Fe}^{4+}}=3.1 \mu_B$ at 4K. On the other hand, Watanabe *et al.*¹⁴⁾ made measurements on single crystals of slightly nonstoichiometric SrFeO_{2.9}, and the magnetic moment was $\mu_{\text{Fe}^{4+}}=5 \mu_B$ in the paramagnetic state and $\mu_{\text{Fe}^{4+}}=2.21 \mu_B$ at 4K. A high spin \rightleftharpoons low spin transition at T_N was suggested accordingly. This disagreement comes from the samples they used and also from the analysis of the intensity data. So, it may be better to refer to another kind of measurement. According to Takeda *et al.*,¹⁵⁾ the high-field magnetization of SrFe_{1-x}Co_xO₃ at 4K, which is ferromagnetic for $0.2 < x \leq 1$, increases linearly with increasing Fe-content and the value extrapolated to SrFeO₃ ($x=0$) corresponds to $\mu_{\text{Fe}^{4+}}=3.73 \mu_B$. This is very close to the spin-only value of $4 \mu_B$ expected from the high spin state. On the other hand, the Mössbauer effect (ME) measurements on SrCo_{0.99}Fe_{0.01}O₃ ($x=0.99$), SrCo_{0.5}Fe_{0.5}O₃ ($x=0.5$),¹⁶⁾ and SrFeO₃¹⁷⁾ showed that the electronic state of the Fe ions remains almost the same: the isomer shift is almost independent of composition, $\approx 0.05 \text{ mms}^{-1}$ at room temperature, and the hyperfine field at 4K varies monotonically as 29.6 T for $x=0.99$, 30.2 T for $x=0.5$, and 33.1 T for $x=0$. Such a possibility that the electronic state of the Fe⁴⁺ ions changes within a composition range of $0 < x \leq 0.2$ to the low spin state is rejected particularly by the absence of a corresponding change in hyperfine field. Thus, the magnetization and ME measurements on SrCo_{1-x}Fe_xO₃ strongly suggest that the Fe⁴⁺ ions in SrFeO₃ are in the high spin state.

SrFeO_3 having been the first stoichiometric phase, the ME measurement by Gallagher *et al.*¹⁷⁾ attracted keen attention. The spectra they obtained were very simple and beautiful as can be seen in Fig. 2. A single narrow absorption line with

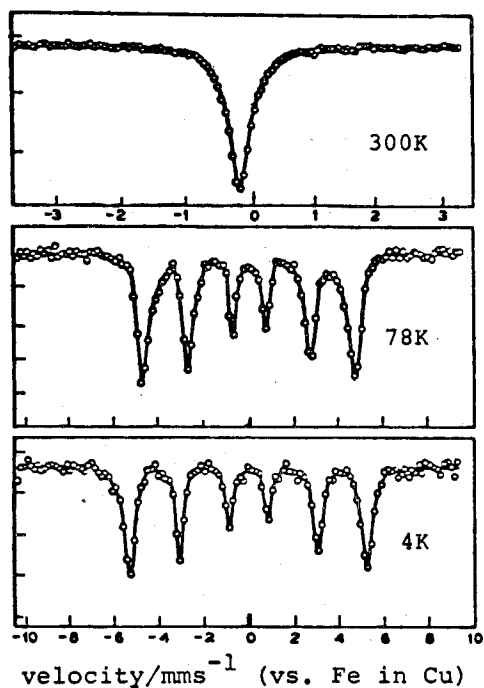


Fig. 2. Mössbauer spectra of SrFeO_3 .¹⁷⁾

an isomer shift (IS) of 0.05 mms^{-1} was observed at room temperature, and a single set of magnetically split absorptions characterized by a magnetic hyperfine field (Hi) of 33.1 T and an IS of 0.146 mms^{-1} appeared at 4K. A quadrupole interaction was not detected. It sometimes happens that structural studies on powdered samples by X-ray or neutron diffraction fail to detect short-range ordered distortions, but the absence of a quadrupole interaction down to 4K rules out this possibility and, hence, the possibility of a stabilization of the high spin state by the Jahn-Teller effect.

The cubic structure and good conductivity retained at least down to 4K and the values of the magnetic moment and the Hi support strongly the quarter-filled narrow σ^* band model.

3.2. CaFeO_3

The girdle-type high pressure apparatus we used to prepare CaFeO_3 is illustrated in Fig. 3. A sandwich type platinum cell was charged with powders of the starting material, $\text{CaFeO}_{2.5}$, and an oxygen generator, CaO_2 or CrO_3 . To prevent the direct reaction of these materials a ZrO_2 disk was interposed. After applying a pressure of 1.5~6 GPa the platinum cell was heated to 1173~1273K to promote

Electronic State of Fe⁴⁺ Ions in Perovskite-type Oxides

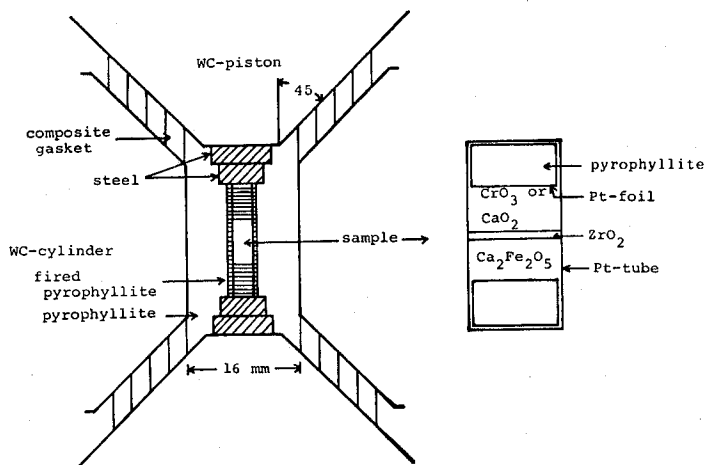


Fig. 3. Girdle-type high pressure apparatus used for the preparation of CaFeO₃.

release of oxygen from the peroxide and absorption by CaFeO_{2.5}. After repeated trials, the most convenient and sufficient conditions were found to be of 2 GPa and 1273K. The oxygen content was checked by the weight change on reducing the product to CaFeO_{2.5} at 1473K in air.³⁾

The crystal data determined by powder X-ray diffraction are given in Table II. The tetramolecular unit cell results from a slight distortion of the perovskite

Table II. Crystal Data for CaFeO₃ and SrFeO₃ at Room Temperature.

Oxide	Symmetry	Lattice Constants	Volume per Molecule
SrFeO ₃ ¹⁾	cubic	$a=0.3850$ nm	5.707×10^{-2} nm ³
CaFeO ₃ ³⁾	tetragonal	$a=0.5325$ nm $c=0.7579$ nm	5.373×10^{-2} nm ³

cell. This seems to be due to an imperfect combination of the ionic radii; the radius of the Ca²⁺ ion, $r(\text{XII Ca}^{2+})=0.134$ nm,⁹⁾ is slightly smaller than that of the O²⁻ ion. Cubic SrTiO₃ and orthorhombic CaTiO₃ afford a parallel pair.

Measurements of magnetic susceptibility and electrical resistivity were made between room temperature and 77K.³⁾ The susceptibility showed a typical anti-ferromagnetic behavior with its maximum at 115K as shown in Fig. 4. We, unfortunately, found difficulty to obtain reproducible resistivity data, which may be due to the small sample volumes, small cracks in the sintered bodies, and contaminations. However, at the present stage, we can say at least that the resistivity at room temperature is ~ 10 Ω cm, which is 10⁴ times that of SrFeO₃ and that the temperature dependence is semiconductive: the difference in resistivity increases with decreasing temperature. In near future these kinds of measurements will be repeated on samples of more suitable volume and better quality.

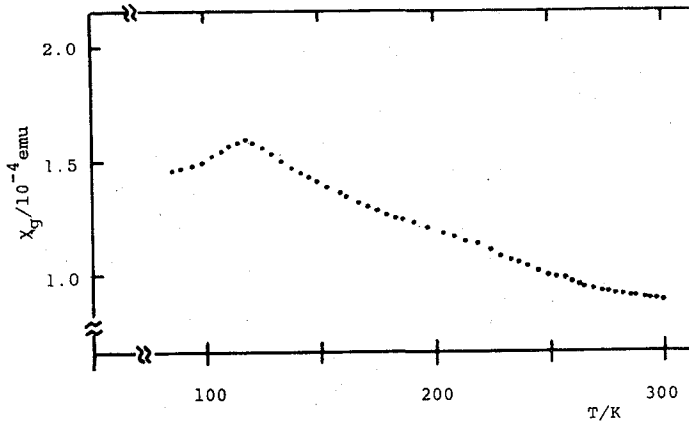


Fig. 4. Temperature dependence of magnetic susceptibility of CaFeO_3 .

The samples used for ME measurements were enriched with ^{57}Fe up to about 10% to compensate the small sample volume. The spectra³⁾ are shown in Fig. 5, and the parameters are given in Table III together with those for SrFeO_3 .¹⁷⁾

A sharp absorption peak without any trace of undesirable absorption by Fe^{3+} ions was observed at room temperature, which assured the proper stoichiometry of our sample. The IS is very close to that of SrFeO_3 , suggesting that the Fe ions in CaFeO_3 and SrFeO_3 have similar electronic states. However, the spectrum at 4K consists of two sets of magnetic hyperfine patterns of equal intensities in sharp

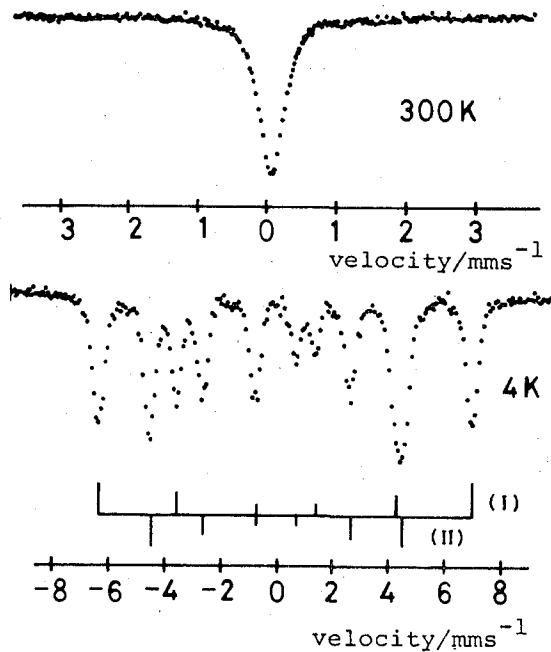


Fig. 5. Mössbauer spectra of CaFeO_3 .

Electronic State of Fe⁴⁺ Ions in Perovskite-type Oxides

 Table III. Mössbauer Effect Parameters for SrFeO₃ and CaFeO₃.

Oxide	<i>IS</i> /mms ⁻¹			<i>Hi</i> /T at 4 K			
	300 K	4 K					
SrFeO ₃ ¹⁷⁾	0.054	0.146		33.1			
CaFeO ₃ ³⁾	0.073	I	II	(I+II)/2	I	II	(I+II)/2
		0.34	0.00	0.17	41.6	27.9	34.8

contrast to that of SrFeO₃. The differences in the parameter values between components I and II are large enough to allow an assignment to Fe ions in different valence states. For this assignment we took the following points into consideration. Firstly, the total s electron density at an ⁵⁷Fe nucleus generally decreases and, hence, the *IS* becomes more positive with increasing d electron number by a shielding effect. Secondly, the polarized s electron density at the nucleus increases and, hence, the absolute value of core-polarization hyperfine field increases with increasing polarized d electron number. Thirdly, the parameter values averaged over components I and II are very close to the corresponding parameters for SrFeO₃. Then, we proposed a very simple charge disproportionation model.¹⁸⁾ At low temperatures a half of the Fe⁴⁺ ions in CaFeO₃ lose one electron to become Fe⁵⁺ ions and the other half catch the electron to become Fe³⁺ ions. In other words, the e_g electrons in the narrow σ* band become localized at a half of the Fe ions: 2Fe⁴⁺ (t_{2g}³σ_g^{*1}) → Fe³⁺(t_{2g}³e_g²) + Fe⁵⁺(t_{2g}³e_g⁰). As a matter of course, component I corresponds to the Fe³⁺ ions and component II to the Fe⁵⁺ ions.

Both parameters for component I are somewhat smaller than the typical values for Fe³⁺ ions at octahedral sites of *IS* ≈ 0.5 mms⁻¹ and *Hi* ≈ 55 T at 0K, but this may be explained by a reduction of the e_g electron density due to the presence of highly charged Fe⁵⁺ ions with empty e_g orbitals in the neighboring sites.

Scholder *et al.*¹⁹⁾ reported in the past oxides of compositions R₃FeO₄ (R=K, Na and Rb) which contain Fe⁵⁺ ions at tetrahedral sites. However, the oxidation state has not been established by proper physical techniques. On the other hand, Müller *et al.*²⁰⁾ detected Fe⁵⁺ ions contained as a dilute impurity in SrTiO₃ by ESR. The magnetic hyperfine constant for the ⁵⁷Fe⁵⁺ ion corresponds to a *Hi* of 28 T, which is in perfect agreement with the value for component II. This agreement supports our assignment strongly, though the agreement should not be taken too seriously because hyperfine field is, generally, influenced by the surroundings.

Because of the rareness of the Fe⁵⁺ state we were eager to collect further confirmations of the charge disproportionation model by studying some related oxide systems rather than to concentrate on CaFeO₃. Then, two series of solid solutions of Ca_{1-x}Sr_xFeO₃ and Sr_{1-y}La_yFeO₃ were prepared. From the first series we expected the existence of a critical Sr content where the e_g electrons become itinerant and, therefore, the spectrum at 4K changes from the CaFeO₃-type to the SrFeO₃-type. This was a reasonable expectation if discrete valence states of Fe³⁺, Fe⁴⁺, and Fe⁵⁺ were assumed. On looking into the ME spectra for the second system

reported by Gallagher and MacChesney,²¹⁾ we became confident that substitution of La^{3+} ions for Sr^{2+} ions induces a similar disproportionation. Then, we expected to observe a reasonable composition dependence of the $\text{Fe}^{3+}/\text{Fe}^{5+}$ ratio.

3.3. $\text{Ca}_{1-x}\text{Sr}_x\text{FeO}_3$.

Samples of compositions $x=0.125, 0.25, 0.5, 0.625,$ and 0.75 were prepared by the same method as was applied to the preparation of CaFeO_3 .²²⁾ The applied pressure was 2.5 GPa and the samples were heated to 1273K.

The substitution of $x \geq 0.125$ makes the structure cubic. The lattice constant increases almost linearly with x as shown in Fig. 6. Magnetic susceptibility measurements indicated that all the compositions are antiferromagnetic.

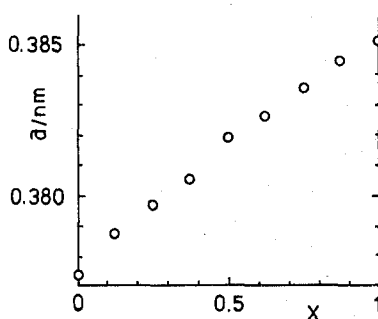


Fig. 6. Composition dependence of lattice constant of $\text{Ca}_{1-x}\text{Sr}_x\text{FeO}_3$. The value for CaFeO_3 is the cubic root of the volume per mole.

The ME spectrum at room temperature consists of a single line for every composition, and the IS of 0.06 mms^{-1} is independent of composition within experimental error, indicating that there is no remarkable change in the electronic state. However, at 4K, we observed an unexpected composition dependence. As can be seen in Fig. 7, there is no sharp change in the character of the spectrum: even $\text{Ca}_{0.25}\text{Sr}_{0.75}\text{FeO}_3$ exhibits double components. Continuously with increasing Sr content, the absorption lines become broader and, at the same time, the differences in the parameters between the double components become smaller. The spectra were computer-analyzed using broadened Lorentzian lines for convenience. Areas of the double components are almost the same for any composition. The parameter values are plotted in Fig. 8. It is quite impressive that the double components merge into one at $x=1$.

These results supported our model in the sense that the Fe^{4+} ions disproportionated into equal numbers of Fe ions having valences higher and lower than 4+ but, at the same time, gave rise to another problem of indistinct, continuous valence.

3.4. $\text{Sr}_{1-y}\text{La}_y\text{FeO}_3$.

Some stoichiometric perovskite phases of the $\text{Sr}_{1-y}\text{La}_y\text{FeO}_3$ system were studied by Gallagher and MacChesney²¹⁾ in the past (this work will be referred to as GM, hereafter). They observed average valence states due to a rapid electron exchange,

Electronic State of Fe⁴⁺ Ions in Perovskite-type Oxides

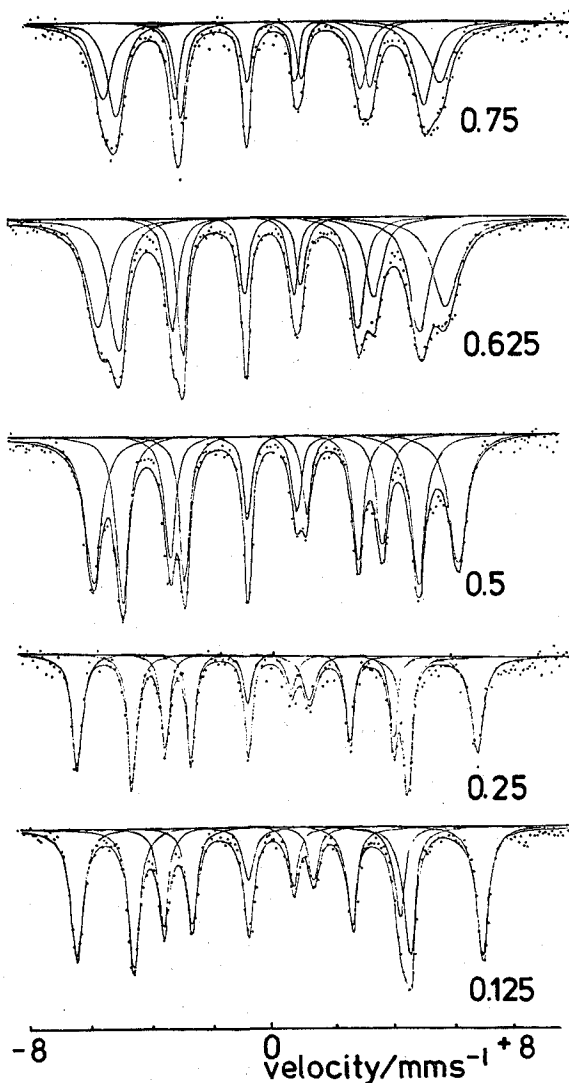


Fig. 7. Mössbauer spectra of Ca_{1-x}Sr_xFeO₃ at 4K.

which may be expressed as Fe^{(4-y)+}, for $y \leq 0.6$ at room temperature. On the other hand, they obtained complex spectra at 4K, which were interpreted as indicating a resolution into the individual valence states of Fe³⁺ and Fe⁴⁺. Sr_{0.6}La_{0.4}FeO₃ particularly exhibited well resolved double components. However, though Fe³⁺/Fe⁴⁺=4/6 for this composition, the intensity ratio of the corresponding components was indicative of Fe³⁺/Fe⁴⁺>1. If a charge disproportionation is supposed to occur instead, the expected ratio of Fe³⁺/Fe⁵⁺=(1+y)/(1-y) should be larger than unity. Then, we repeated ME measurements on this system expecting an application of our model.²³⁾

Samples of compositions of $y=0.1, 0.2, 0.3, 0.5,$ and 0.6 were treated finally under oxygen pressures of 100~150 MPa at 673~873K for 170~500 hr depending

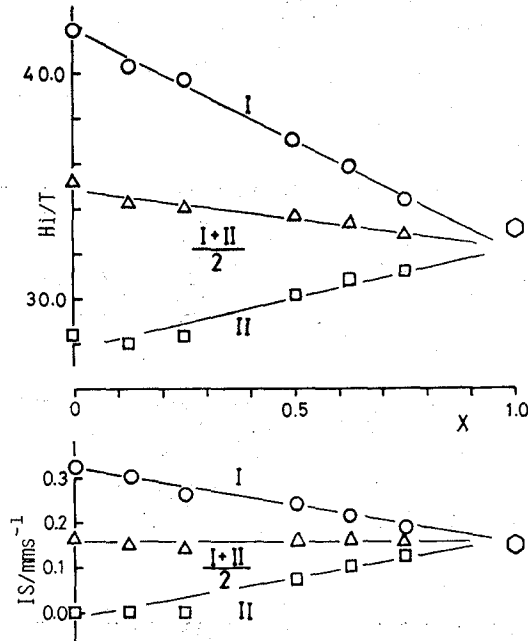


Fig. 8. Composition dependence of isomer shift and magnetic hyperfine field of $\text{Ca}_{1-x}\text{Sr}_x\text{FeO}_3$ at 4 K.

upon composition. The crystal data obtained by powder x-ray diffraction measurements are given in Table IV. The data are in excellent agreement with those by GM except for the case of $y=0.3$ to which GM assigned cubic symmetry. The temperature dependence of the magnetization is shown in Fig. 9. Antiferromagnetism with or without parasitic ferromagnetism, depending upon crystalline symmetry, was observed. The temperature of a magnetic anomaly indicated as T_m in Fig. 9, is also given in Table IV. As will be described later, the ME measurements on

Table IV. Crystal Data and T_m for $\text{Sr}_{1-y}\text{La}_y\text{FeO}_3$.

Composition y	Symmetry	Lattice Constants	Volume	T_m
0.1	cubic	$a=0.38590$ nm	5.747×10^{-2} nm ³	114 K
0.2	cubic	$a=0.38652$ nm	5.775×10^{-2} nm ³	139 K
0.3	rhombohedral	$a=0.3873$ nm $\alpha=90.05^\circ$	5.810×10^{-2} nm ³	199 K
0.5	rhombohedral	$a=0.3889$ nm* $\alpha=90.26^\circ$ *	5.882×10^{-2} nm ³	230 K
0.6	rhombohedral	$a=0.3896$ nm* $\alpha=90.333^\circ$ *	5.913×10^{-2} nm ³	>300 K

* The data given by GM⁽²¹⁾ explain very well the diffraction pattern of our sample.

Electronic State of Fe⁴⁺ Ions in Perovskite-type Oxides

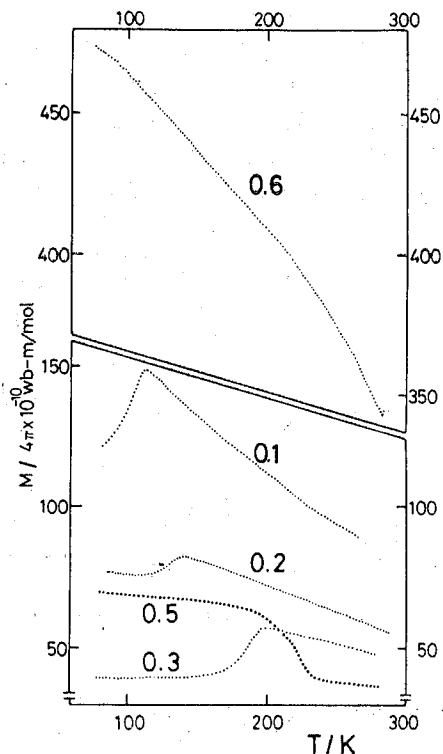


Fig. 9. Temperature dependence of magnetization of $\text{Sr}_{1-y}\text{La}_y\text{FeO}_3$.

compositions of $y=0.3$ and 0.5 revealed that these anomalies do not correspond to a normal second order transition.

Electrical resistivity was measured for the compositions of $y=0.3$ and 0.5 . As can be seen in Fig. 10 there exist two temperature ranges where the resistivity shows a normal semiconductive temperature dependence with a fixed activation energy for both compositions. Sandwiched between these is an unusual range, the high temperature end of which is close to the T_m .

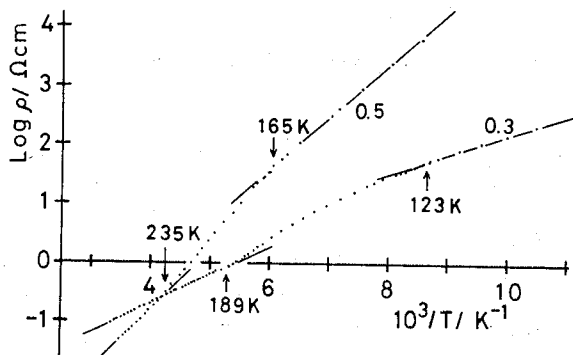


Fig. 10. Temperature dependence of electrical resistivity of $\text{Sr}_{0.7}\text{La}_{0.3}\text{FeO}_3$ ($y=0.3$) and $\text{Sr}_{0.5}\text{La}_{0.5}\text{FeO}_3$ ($y=0.5$).

The ME spectra at room temperature are shown in Fig. 11. In agreement with GM we observed a single absorption peak or a single quadrupole doublet for $y \leq 0.5$. The spectrum for $y=0.6$ has a magnetically perturbed background and was not computer-analyzed. However, the central absorption line is quite similar to that for $y=0.5$. The IS increases linearly with y as plotted in Fig. 12: the Fe ions have an averaged e_g electron number of $(1+y)/\text{Fe}$.

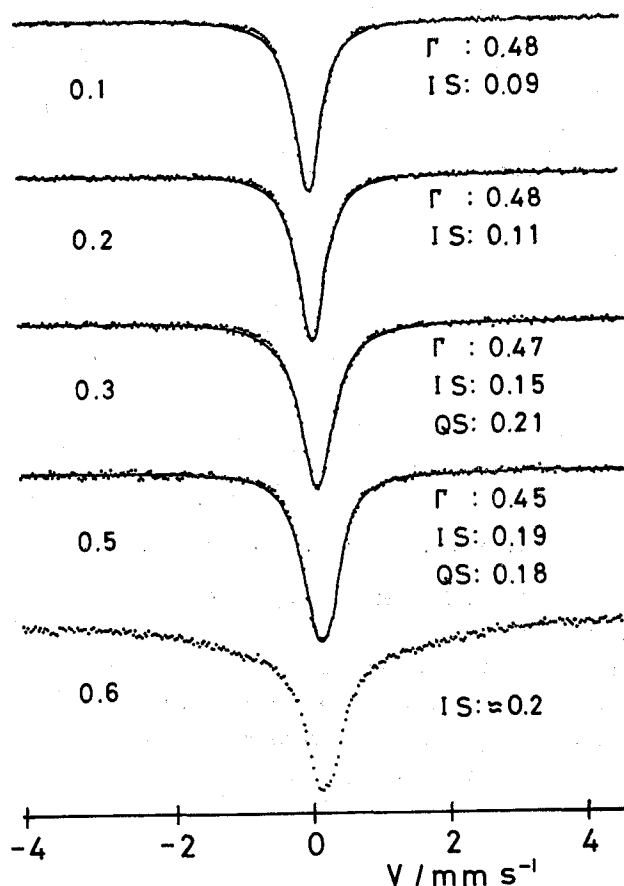


Fig. 11. Mössbauer spectra of $\text{Sr}_{1-y}\text{La}_y\text{FeO}_3$ at 300 K.

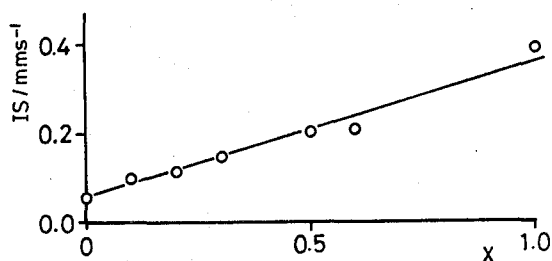


Fig. 12. Composition dependence of isomer shift of $\text{Sr}_{1-y}\text{La}_y\text{FeO}_3$ at 300 K.

A typical disproportionation meeting to our expectations was observed for $\text{Sr}_{0.7}\text{La}_{0.3}\text{FeO}_3$ at 4K. As shown in Fig. 13, the absorption lines are sharp and are well-resolved. The IS 's and Hi 's for the double components are rather close to those for CaFeO_3 . The intensity ratio is, however, not unity as it is for CaFeO_3 , but is 66:34, just fitting the composition of $\text{Sr}_{0.7}\text{La}_{0.3}\text{Fe}_{0.65}^{3+}\text{Fe}_{0.35}^{5+}\text{O}_3$. Quite a similar, well-resolved spectrum was reported for the composition of $y=0.4$ by GM. The intensity ratio was not reported, but it seems to be favorable for our model.

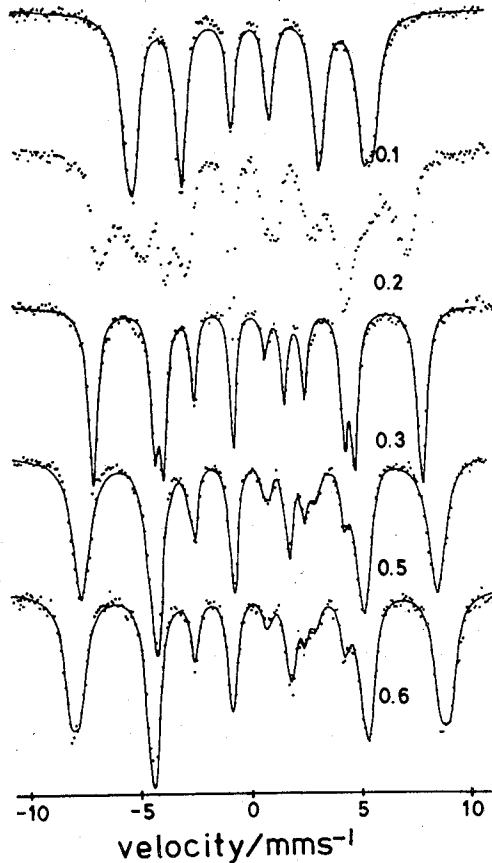


Fig. 13. Mössbauer spectra of $\text{Sr}_{1-y}\text{La}_y\text{FeO}_3$ at 4 K.

Resolution into two components becomes poorer with increasing Sr content as noted in $\text{Ca}_{1-x}\text{Sr}_x\text{FeO}_3$, too. For $y=0.1$, the components are so close to each other that the spectrum looks almost like a single set of magnetic pattern.

On the other hand, as the Sr content is increased, three or more components appear to make the spectra quite complex.²⁴⁾ Though the presence of more than two components is beyond our model, we suggest that these can be divided into two groups according to the parameter values and that the relative intensity is close to the expected value as seen in Table V.

Table V. Mössbauer Data for $\text{Sr}_{1-y}\text{La}_y\text{FeO}_3$ at 4 K.

Composition y	Component	IS (mms^{-1})	H (T)	I (%)
0.1	I	0.20	34.5	56
	II	0.12	32.8	44
	av.	0.16	33.6	
0.2	I	~ 0.33	~ 43	~ 60
	II	~ 0.05	~ 31	~ 40
	av.	~ 0.19	~ 37	
0.3	I	0.36	46.0	66
	II	-0.05	26.9	34
	av.	0.16	36.5	
0.5	I	0.44	50.5	72
	II	0.00	26.2	13
	II'	0.10	29.8	15
	av.	0.25	39.3	
0.6	I	0.44	54.2	39
	I'	0.42	50.4	37
	II	-0.05	26.6	14
	II'	0.12	29.3	10
	av.	0.23	40.1	

3.5. CaFeO_3 and $\text{Sr}_{0.7}\text{La}_{0.3}\text{FeO}_3$ at Intermediate Temperatures.

We have described the composition and temperature dependence of the electronic state of the "Fe⁴⁺" ions up to now and emphasized the disproportionation in CaFeO_3 and $\text{Sr}_{0.7}\text{La}_{0.3}\text{FeO}_3$ by showing the ME spectra at room temperature and 4K. It has been very interesting for us, as a matter of course, to study these oxides in the intermediate temperature range.

Some of the spectra for CaFeO_3 at various temperatures between 300K and 77K are shown in Fig. 14.^{24,25)} As can be seen most clearly in the spectrum at 154K, a pair of peaks of equal intensities appeared below about 290K. These double peaks can be interpreted in two ways; one is a temperature-dependent quadrupole interaction and the other is the onset of the disproportionation. We take the latter considering the following points. Firstly, though the crystal is slightly distorted from cubic symmetry even at 300K, any sign of quadrupole interaction cannot be detected in the well-resolved spectrum at 4K. The quadrupole interaction is probably negligibly small below 300K. Secondly, the separation between the double peaks gets saturated at about 160K as shown in Fig. 15a, and the value of 0.32 mms^{-1} is coincident with the difference in IS between the Fe^{3+} and Fe^{5+} ions at 4K. The peak positions, namely, the IS 's of the Fe^{3+} and Fe^{5+} ions at 154K are more negative by $\approx 0.05 \text{ mms}^{-1}$ than those at 4K, which can be explained by the second order Doppler effect.

Electronic State of Fe⁴⁺ Ions in Perovskite-type Oxides

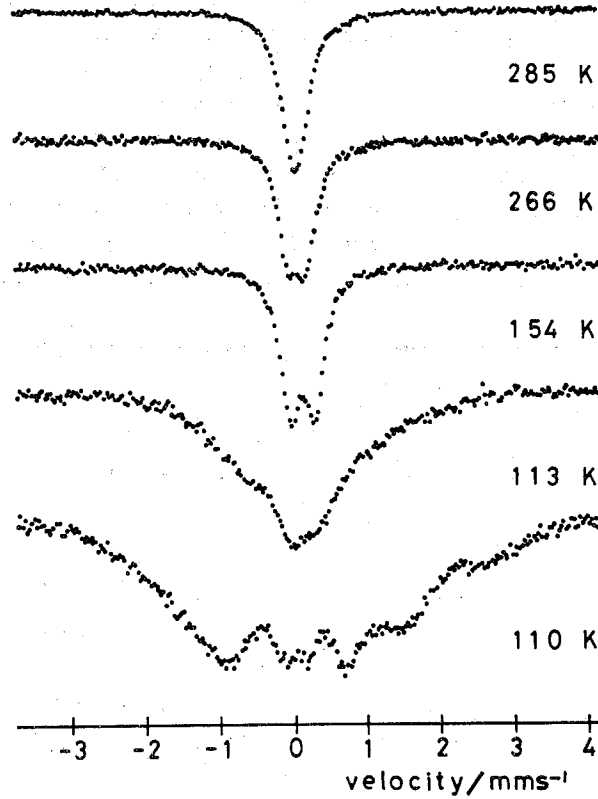


Fig. 14. Mössbauer spectra of CaFeO₃ at intermediate temperatures.

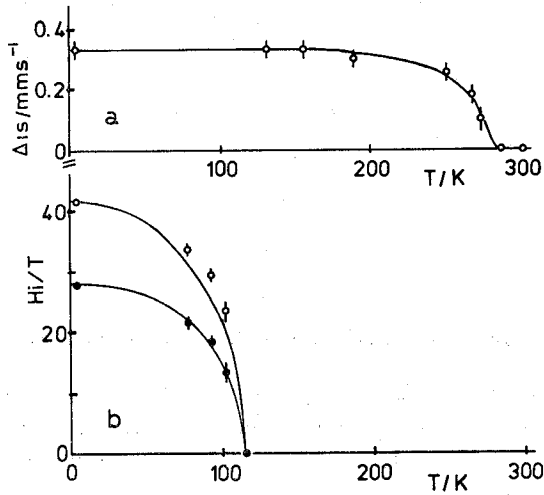


Fig. 15. (a) Temperature dependence of the difference in isomer shift between the two kinds of Fe ions in CaFeO₃. (b) Temperature dependence of the magnetic hyperfine fields of the Fe³⁺ and Fe⁴⁺ ions in CaFeO₃.

The H_i 's plotted in Fig. 15b indicate a normal second order transition. Thus, we conclude that CaFeO_3 shows a transition from its paramagnetic average valence phase (Pa -phase) to the mixed valence phase (Pm) at 290K and, next, a second order transition to the antiferromagnetic mixed valence phase (Am) at 115K. It is noteworthy that the disproportionation proceeds passing through the temperature-dependent intermediate state as can be seen clearly in Fig. 15a.

$\text{Sr}_{0.7}\text{La}_{0.3}\text{FeO}_3$ shows quite a different behavior.²³⁾ A paramagnetic and an antiferromagnetic pattern are superimposed over a wide temperature range as shown in Fig. 16. It should be noted that the resolution into double components

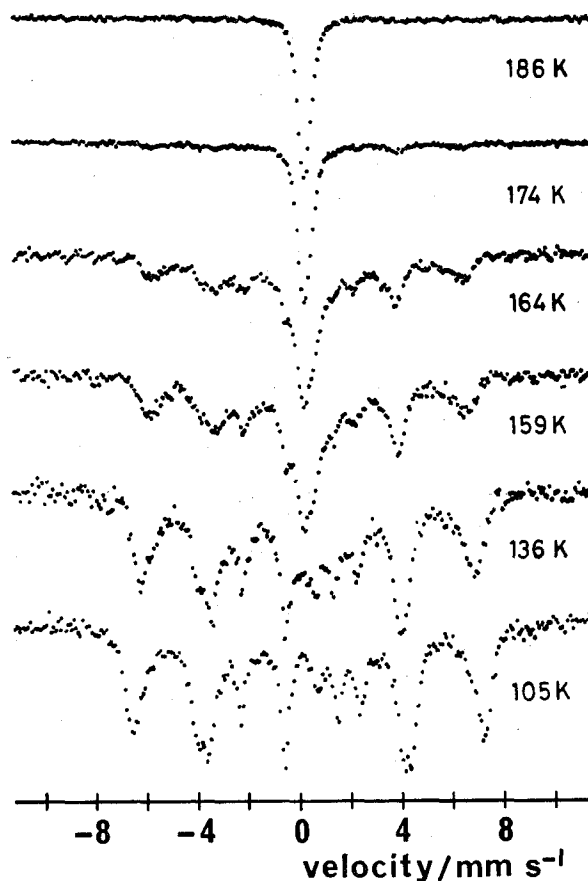
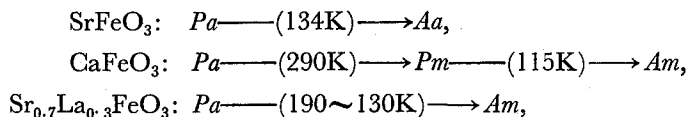


Fig. 16. Mössbauer spectra of $\text{Sr}_{0.7}\text{La}_{0.3}\text{FeO}_3$ at intermediate temperatures.

can be seen only in the antiferromagnetic pattern. Its intensity decreases with increasing temperature to vanish asymptotically at the T_m , the temperature of the magnetic and electrical anomaly. The magnetic splittings remain, however, large even at this temperature. This observation indicates that below the T_m there appear domains in the crystal making a first-order transition from the Pa -phase to the Am phase and that the total volume becomes full at about 130K. The transition temperature might be so susceptible to a locally fluctuating La content that these phases

coexist over the wide temperature range. Spectra of quite a similar character were obtained from Sr_{0.5}La_{0.5}FeO₃ and also from Ca_{0.5}Sr_{0.5}FeO₃. The anomalies detected by the magnetic and electrical measurements for these oxides should not be taken as indicating a normal second order antiferromagnetic transition.

The types of transition we have observed are summarized below.



where *P*, *A*, *a*, and *m* stand for paramagnetic, antiferromagnetic, average valence phase, and mixed valence phase, respectively.

4. SUMMARY

The Fe⁴⁺ ions in SrFeO₃ take the high spin state of $t_{2g}^3 e_g^1$, and the e_g electrons are accommodated in the σ^* band, which is narrow enough to allow polarization of the electrons. The quarter-filled, narrow σ^* band state is stable at least down to 4K.

When the Sr ions are completely replaced by Ca ions to form CaFeO₃, the σ^* band state becomes unstable at 290K, and the Fe⁴⁺ ions disproportionate into equal numbers of Fe³⁺ and Fe⁵⁺ ions passing through temperature-dependent intermediate valence states.

Substitution of La³⁺ ions for the Sr²⁺ ions to form Sr_{1-y}La_yFeO₃ leads to an increase in the e_g electron number from unity to $(1+y)/\text{Fe}$. These additional electrons are also accommodated in the σ^* band so that all the Fe ions take composition-dependent, average valence state. However, at low temperatures the first-order transition to the antiferromagnetic, mixed valence phase containing Fe³⁺ and Fe⁵⁺ ions of a ratio of $(1+y)/2 : (1-y)/2$ occurs for $y=0.3 \sim 0.4$.

In Fig. 17 the *IS*- and *Hi*-values for Ca_{1-x}Sr_xFeO₃ and Sr_{1-y}La_yFeO₃ at 4K are plotted. Figure 17a gives the values for the individual components, and Fig. 17b the averaged values corresponding to the virtual Fe⁴⁺ states. It is impressive that both these parameters take a wide range of continuous values keeping a beautiful correlation between them. On the other hand, the averaged values show a good convergence around the point of $IS=0.15 \text{ mms}^{-1}$ and $Hi=33 \text{ T}$, which is the point for SrFeO₃. Therefore, the chemical formulas appropriate at 4K are Ca_{1-x}Sr_xFe_{0.5}^(3+ δ)Fe_{0.5}^(5- δ)O₃ and Sr_{1-y}La_yFe_{(1+y)/2}^(3+ δ)Fe_{(1-y)/2}^(5- δ)O₃, where both δ and δ increase to unity with increasing Sr content.

It is interesting to point out here the following effects of substitution. CaFeO₃ has a smaller volume per molecule than that of SrFeO₃, and, hence, the Fe-O-Fe bond angle may be decreased to 150~160°, as can be roughly estimated by comparing the lattice constants. This bending would reduce the σ^* band width and accordingly would make the electronic state susceptible to perturbations. On the other hand, the substitution of the La³⁺ ions to form Sr_{0.7}La_{0.3}FeO₃ leads to an increase in the e_g electron number to 1.3/Fe, which would also give rise to an instability

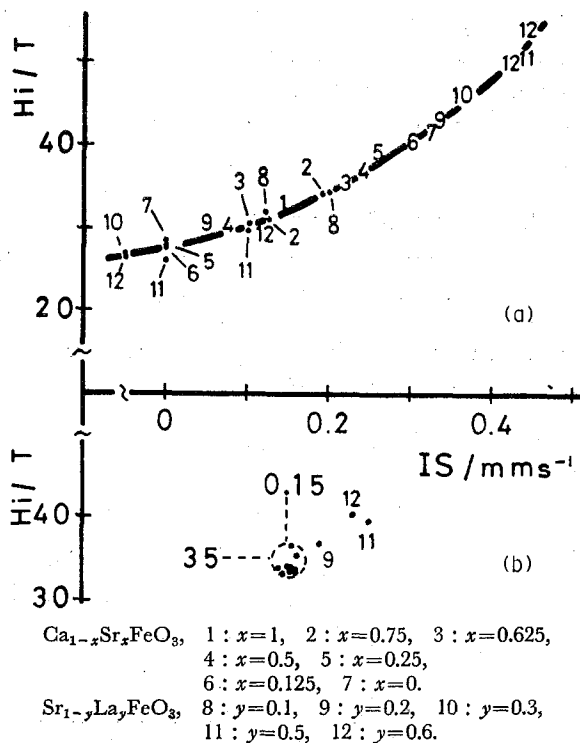


Fig. 17. Mössbauer data for $Ca_{1-x}Sr_xFeO_3$ and $Sr_{1-y}La_yFeO_3$ at 4 K. (a) Data for individual components. (b) Data for the virtual Fe^{4+} state.

of the σ^* band due to increased electron correlation. For both oxides the low temperature phase contains Fe^{3+} and Fe^{5+} ions which are very stable in an octahedral field. The Fe^{3+} ions tend, quite naturally, to be surrounded by the Fe^{5+} ions and *vice versa*; at the same time, the O^{2-} ions would be shifted towards the more highly charged ions. So, it seems to be the coupling of the electronic system with such a phonon mode that induces the phase transition. Our powder X-ray diffraction measurement on $CaFeO_3$ down to 77K, however, did not detect any sign of such an ordered arrangement of the Fe ions, and now we are making use of electron diffraction with which it would be easier to find even a short range ordering.

We have focused our attention only on the two series of oxides. However, we can mention some other interesting oxides each showing a similar phenomenon such as $Sr_3Fe_2O_{6.9}$, $SrFeO_{2.85}$, $BaFeO_{2.95}$ ^{18,26)} and $Ca_{1-z}La_zFeO_3$ ^{27,28)} As can be most clearly seen in $SrFeO_{2.85}$, oxygen deficiency also can induce a disproportionation.²⁶⁾ By the way, interesting to compare with are the oxides prepared and characterized recently by Demazeau *et al.*,^{6,29)} $M_{0.5}La_{1.5}Li_{0.5}Fe_{0.5}^{4+}O_4$ ($M=Ca, Sr, Ba$) of the K_2NiF_4 structure and $LaLi_{0.5}Fe_{0.5}^{5+}O_3$ of the perovskite structure; Fe^{4+} ions take a localized, high spin state in the former and a high concentration of Fe^{5+} ions are stabilized in the latter.

As described above oxides of the perovskite-type structure and of some related

structures containing highly charged Fe ions present a very interesting field of research from the viewpoints of physics, chemistry, theory, and experiment. We hope that further researches open a way to practical use of these oxides.

ACKNOWLEDGMENTS

The original works were made while the authors, M.T. and Y.T., belonged to Konan University and Nagoya University, respectively. They greatly appreciate discussions with and encouragements by Professor N. Nakanishi, Mr. J. Kawachi (Konan University), Professor S. Naka (Nagoya University), Professors T. Takada, Y. Bando, and T. Shinjo (Kyoto University).

REFERENCES

- (1) J.B. MacChesney, R.C. Sherwood, and J.F. Potter, *J. Chem. Phys.*, **43**, 1907 (1965).
- (2) F. Kanamaru, H. Miyamoto, Y. Miura, M. Koizumi, M. Shimada, and S. Kume, *Mat. Res. Bull.*, **5**, 257 (1970).
- (3) Y. Takeda, S. Naka, M. Takano, T. Shinjo, T. Takada, and M. Shimada, *ibid.*, **13**, 61 (1978).
- (4) J.B. MacChesney, H.J. Williams, R.C. Sherwood, and J.F. Potter, *ibid.*, **1**, 113 (1966).
- (5) P.K. Gallagher, J.B. MacChesney, and D.N.E. Buchanan, *J. Chem. Phys.*, **45**, 2466 (1966).
- (6) G. Demazeau, N. Chevreau, L. Fournes, J.-L. Soubeyroux, Y. Takeda, M. Thomas, and M. Pouchard, *Rev. Chim. Min.*, **20**, 155 (1983).
- (7) J.B. MacChesney, J.F. Potter, R.C. Sherwood, and H.J. Williams, *J. Chem. Phys.*, **43**, 3317 (1965).
- (8) T. Ichida, *Bull. Chem. Soc. Japan*, **46**, 1591 (1973) and *J. Solid State Chem.*, **7**, 308 (1973).
- (9) R.D. Shannon, *Acta Cryst.*, **A32**, 751 (1976).
- (10) J.B. Goodenough and J.M. Longo, "Landolt-Bornstein Tabellen Neue Serie", III/4a, Springer-Verlag, Berlin, 1970, p. 126.
- (11) J.B. Goodenough in "Progress in Solid State Chemistry", Vol. 5, H. Reiss Ed., Pergamon Press, Oxford, 1971, Ch. 4.
- (12) T. Takeda, Y. Yamaguchi, and H. Watanabe, *J. Phys. Soc. Japan*, **33**, 967 (1972).
- (13) T. Takeda, S. Komura, and N. Watanabe in "FERRITES: Proc. Int. Conf. Sept.-Oct. 1980, Japan", H. Watanabe, S. Iida, and M. Sugimoto Ed., Center for Academic Publication, Japan, 1981, p. 385.
- (14) H. Watanabe, H. Oda, E. Nakamura, Y. Yamaguchi, and H. Takei, *ibid.*, p. 381.
- (15) T. Takeda, S. Komura, and H. Fujii, *J. Mag. Mag. Mater.* **31-34**, 797 (1983).
- (16) T. Shinjo, M. Takano, H. Taguchi, and M. Shimada, *J. Phys. Colloq.*, **41**, C1-157 (1980).
- (17) P.K. Gallagher, J.B. MacChesney, and D.N.E. Buchanan, *J. Chem. Phys.*, **41**, 2429 (1964).
- (18) M. Takano, N. Nakanishi, Y. Takeda, S. Naka, and T. Takeda, *Mat. Res. Bull.*, **12**, 923 (1977).
- (19) R. Scholder, *Bull. Soc. Chim. Fr.*, 1112 (1965).
- (20) K.A. Müller, Th von Waldkirch, W. Berlinger, and B.W. Faughnan, *Solid State Comm.*, **9**, 1097 (1971).
- (21) P.K. Gallagher and J.B. MacChesney, *Symp. Faraday Soc.*, **1**, 40 (1968).
- (22) Y. Takeda, S. Naka, M. Takano, and N. Nakanishi, *J. Phys. Colloq.*, **40**, C2-331 (1979).
- (23) M. Takano, J. Kawachi, N. Nakanishi, and Y. Takeda, *J. Solid State Chem.*, **39**, 75 (1981).
- (24) M. Takano, N. Nakanishi, Y. Takeda, and S. Naka, *J. Phys. Colloq.*, **40**, C2-313 (1979).
- (25) T. Shinjo, N. Hosoi, T. Takada, M. Takano, and Y. Takeda in "FERRITES: Proc. Int. Conf. Sept.-Oct. 1980, Japan", H. Watanabe, S. Iida, and M. Sugimoto Ed., Center for Academic Publication, Japan, 1981, p. 383.
- (26) M. Takano, N. Nakanishi, Y. Takeda, and T. Shinjo, *ibid.*, p. 389.
- (27) Y. Takeda, K. Kajiura, S. Naka, and M. Takano, *ibid.*, p. 414.
- (28) S. Komornicki, L. Fournes, J.-C. Grenier, F. Menil, M. Pouchard, and P. Hagenmuller, *Mat. Res. Bull.*, **16**, 969 (1981).
- (29) D. Demazeau, B. Buffat, F. Menil, L. Fournes, M. Pouchard, J.M. Dance, P. Fabritchnyi, and P. Hagenmuller, *Mat. Res. Bull.*, **16**, 1465 (1981).